

# A Consistent Rain Flag for Ocean Vector Winds

Bryan W. Stiles and Alexander G. Fore

Jet Propulsion Laboratory, California Institute of Technology



## ABSTRACT

The difference in C-band and Ku-band retrieved wind speeds is a figure of merit that can be used to quantify rain contamination. Because C-band winds are much less sensitive to rain than Ku-band scatterometers [Nie and Long, 2007], increasing rain contamination causes the retrieved speeds of the two sensors to diverge. We outline a method for estimating the difference in Ku- and C-band speeds from Ku-band data alone, using the absolute value of the speed difference estimate to flag for rain contamination, and subtracting the estimated speed difference from Ku-band speeds to correct them for rain. Preliminary estimates of the flagging and speed correction accuracy of this method are shown below. The estimated Ku-band/C-band speed difference may also be computed from data available from the two currently operating C-band scatterometers (ASCAT-A and ASCAT-B) and microwave radiometers that share the same satellite platforms, and used to consistently flag C-band scatterometer winds. By utilizing different thresholds on the speed difference estimate, users can flag the appropriate amount of rain contaminated data for their application for each of the two scatterometer types independently, or they can choose a single threshold to regularize the sampling of the wind fields from the two sensors. We plan to produce and publicly distribute speed difference estimates co-registered with existing swath-based wind products (Level 2B) for ASCAT-A, ASCAT-B, ScatSAT, and QuikSCAT. For ScatSAT and QuikSCAT rain corrected wind speeds will be included in the distributed products. Along with the products we will also provide estimates of the speed and zonal and meridional wind component errors for each sensor as a function of estimated C-band/Ku-band wind speed difference. We will characterize the errors in both Ku-band and C-band winds as a function of estimated Ku-band/C-band speed difference using triple collocation methods [Vogelzang et al, 2012] with buoys and NWP winds. Users can utilize the estimated errors to determine the thresholds to use to exclude the appropriate amount of rain-contaminated data for their desired applications. We also plan to compare error estimates and flag values with coincident microwave radiometer rain rates to better understand the effect of rain on scatterometer winds. An important part of the characterization is to find wind regimes where C-band and Ku-band wind speeds differ even in the absence of rain. Such differences can occur due to reduced sensitivity for C-band backscatter at high winds [Fernandez et al, 2006], differing SST effects on C-band and Ku-band backscatter [Wang et al, 2017], and inconsistencies in Ku-band and C-band GMFs.

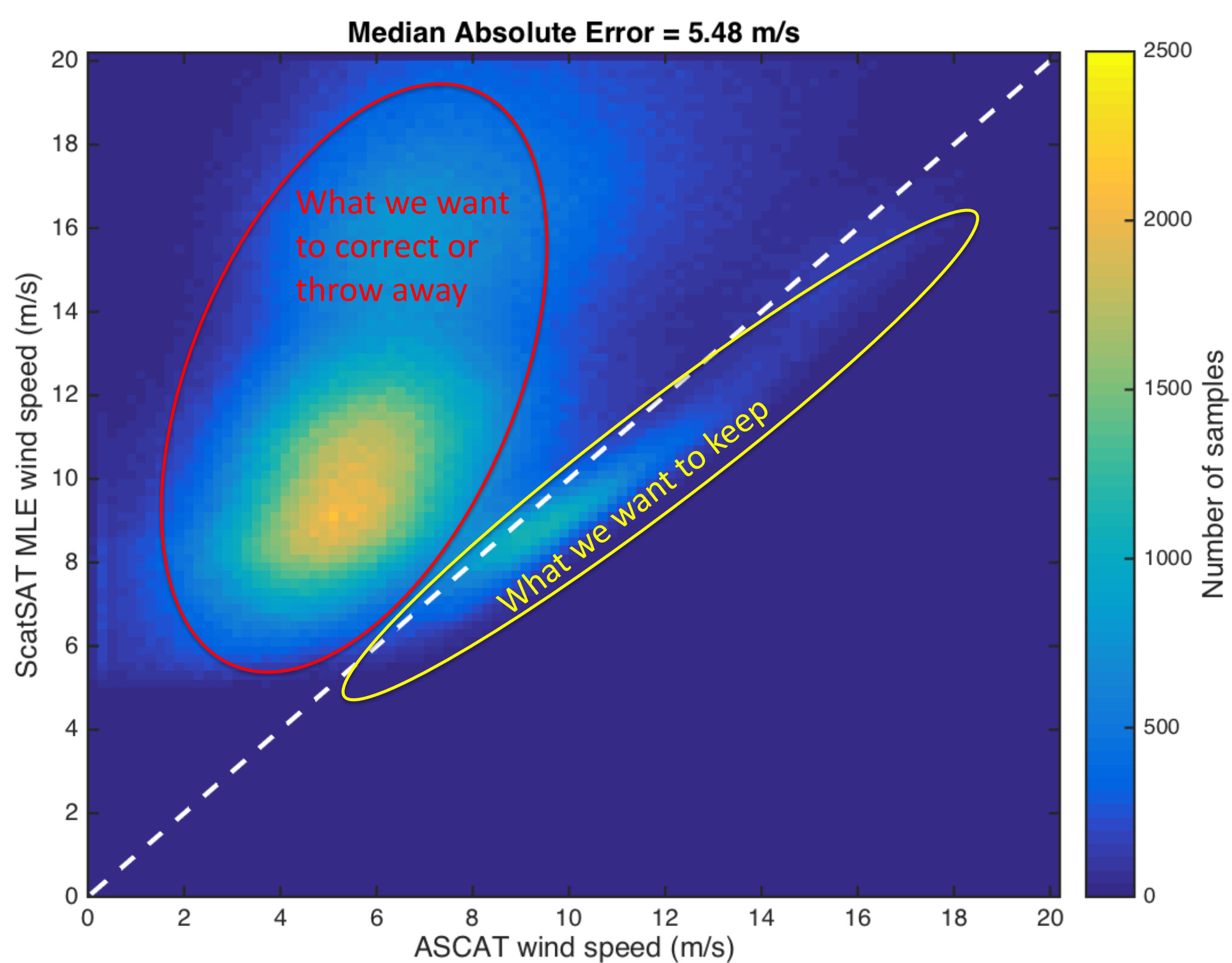


**Figure 1.** Two-dimensional histogram of nominally rain flagged ScatSAT and co-located ASCAT wind speeds retrieved by JPL without correction for rain. Data shown was that determined to be rain-impacted and selected for correction using the nominal JPL QuikSCAT rain correction technique described in [Stiles and Dunbar, 2010] and [Fore et al, 2014]. ASCAT windspeeds are on the x-axis. ScatSAT wind speeds are on the y-axis. Colors represent the number of occurrences. The white line is the one-to-one line representing a perfect match between ScatSAT and ASCAT wind speeds. The data has a bimodal distribution. The elongated patch of data just below the one-to-one line is comprised of "false alarm" co-locations with good agreement between ASCAT and ScatSAT. The wider blob above the line has no such agreement.

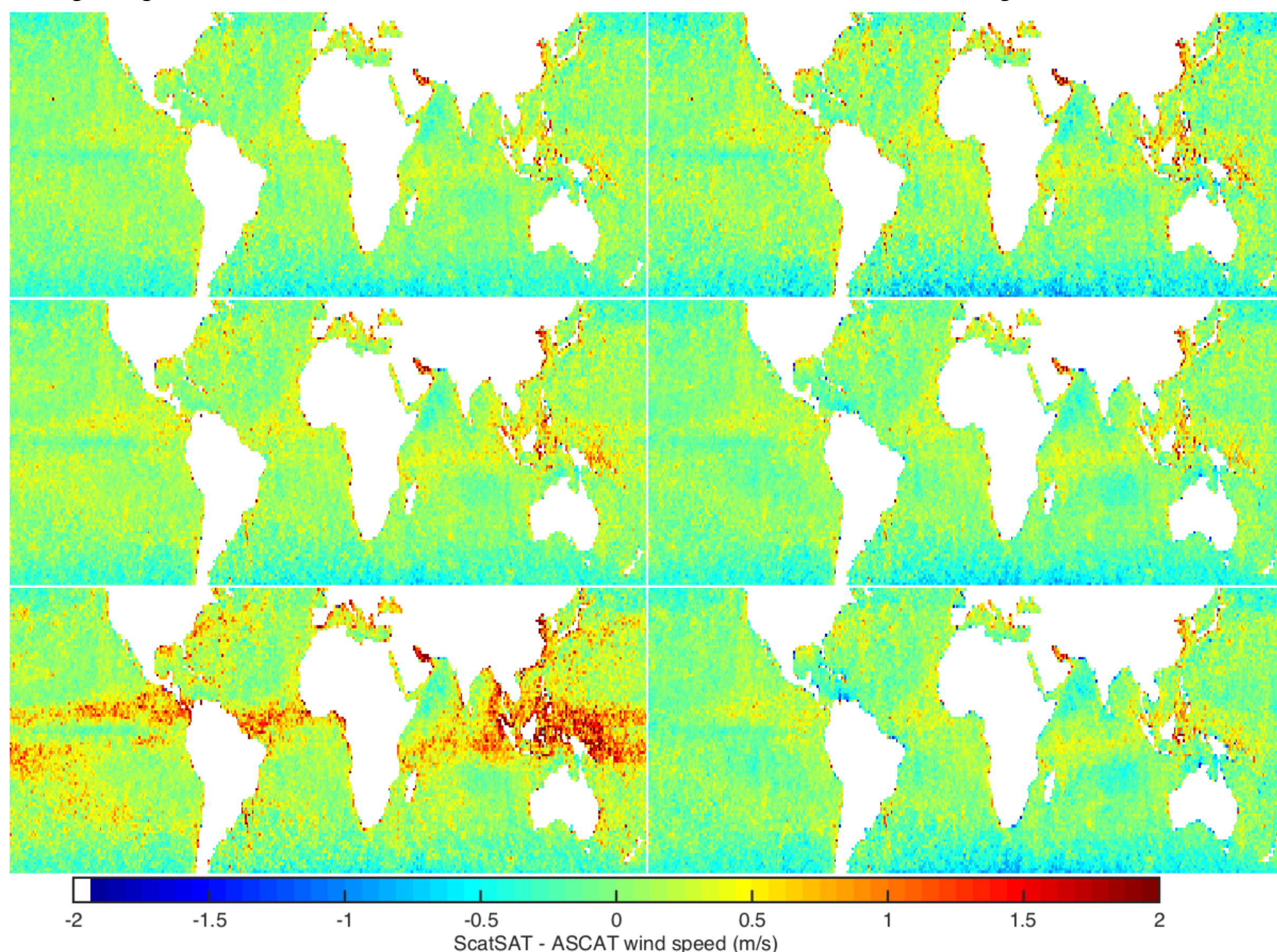


**Figure 3.** ScatSAT-ASCAT wind speeds for 3 different flagging thresholds. Top panels: 0.2 m/s flag threshold, 15% flagged. Middle panels, 1.5 m/s flag threshold, 5% flagged. Bottom panels: 7.8 m/s flag threshold, 1% flagged. Panels on left are uncorrected ScatSAT speeds. Panels on right are corrected. Table 1 shows statistics for top left and bottom right panels.

**Table 1.** ScatSAT-ASCAT wind statistics for most and least conservative flagging cases illustrated in Fig 3

Case Description	Statistics of all data that passed flag (Bias, standard deviation)	Statistics of worst percentile of data that passed flag
Most conservative case (Top left Fig 3) 15% of data rejected Speeds not corrected for rain contamination.	Speed (-0.01 m/s, 0.85 m/s) Zonal (0.06 m/s eastward, 1.26 m/s) Meridional (0.03 northward, 1.38 m/s)	Speed (+0.15 m/s, 1.04 m/s) Zonal (0.01 m/s westward, 1.55 m/s) Meridional (0.04 northward, 1.49 m/s)
Most aggressive case (Bottom right Fig 3) 1% of data rejected Speed correction applied.	Speed (+0.04 m/s, 0.98 m/s) Zonal (0.04 m/s eastward, 1.45 m/s) Meridional (0.03 northward, 1.51 m/s)	Speed (+0.01 m/s, 2.06 m/s) Zonal (0.40 m/s eastward, 3.05 m/s) Meridional (0.22 m/s northward, 3.43 m/s)

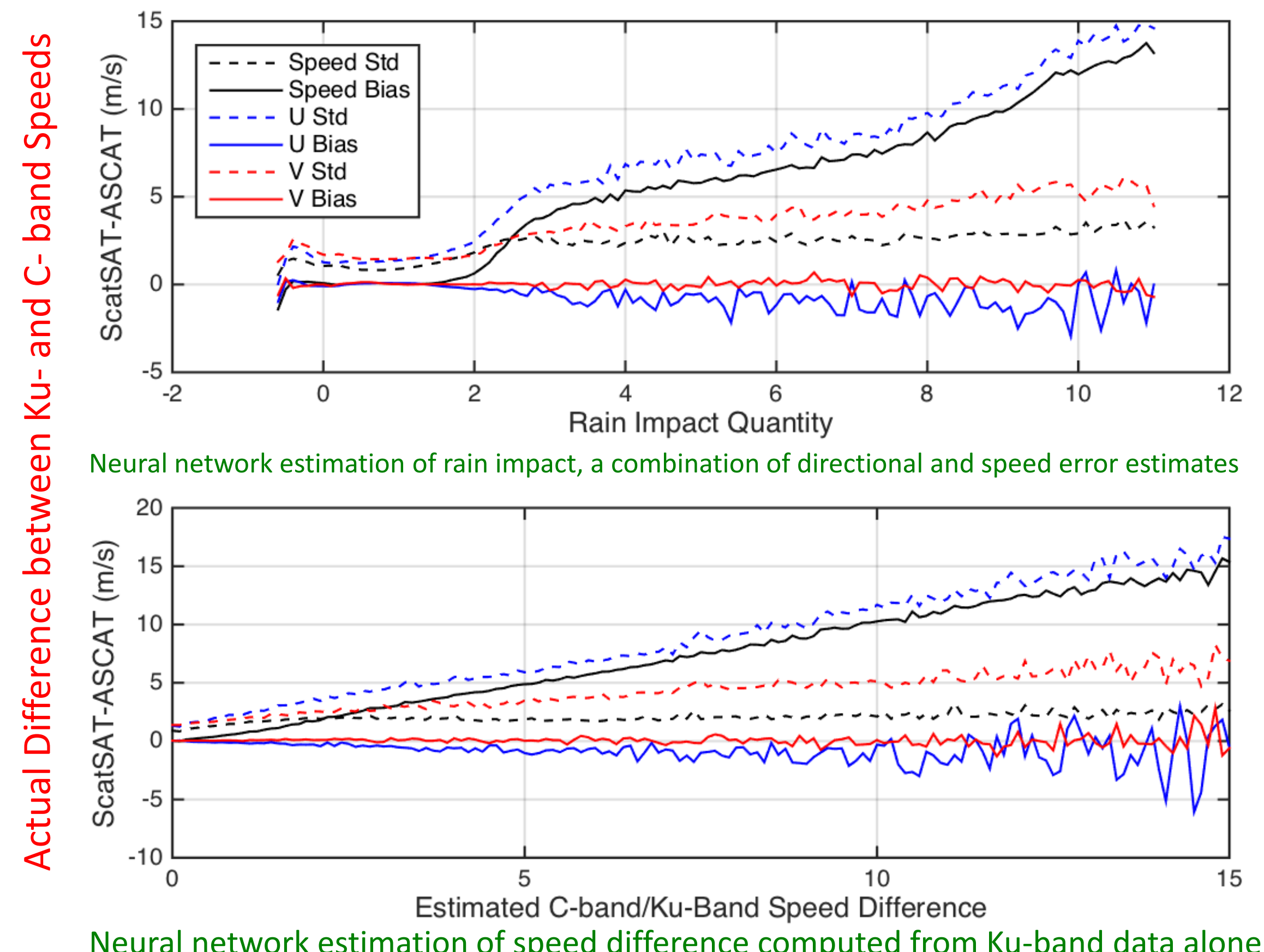


**Figure 2.** Comparison of preliminary version of proposed rain flag with current rain impact quantity. The top panel plots wind difference metrics between uncorrected ScatSAT speeds and ASCAT speeds vs. rain impact quantity. The bottom panel plots the same metrics vs. the proposed rain contamination metric, the absolute value of the estimated C-band/Ku-band speed difference. Black solid lines are speed biases (ScatSAT-ASCAT). Blue and red solid lines are zonal (u) wind component and meridional (v) wind component biases, respectively. Dashed lines are standard deviations.

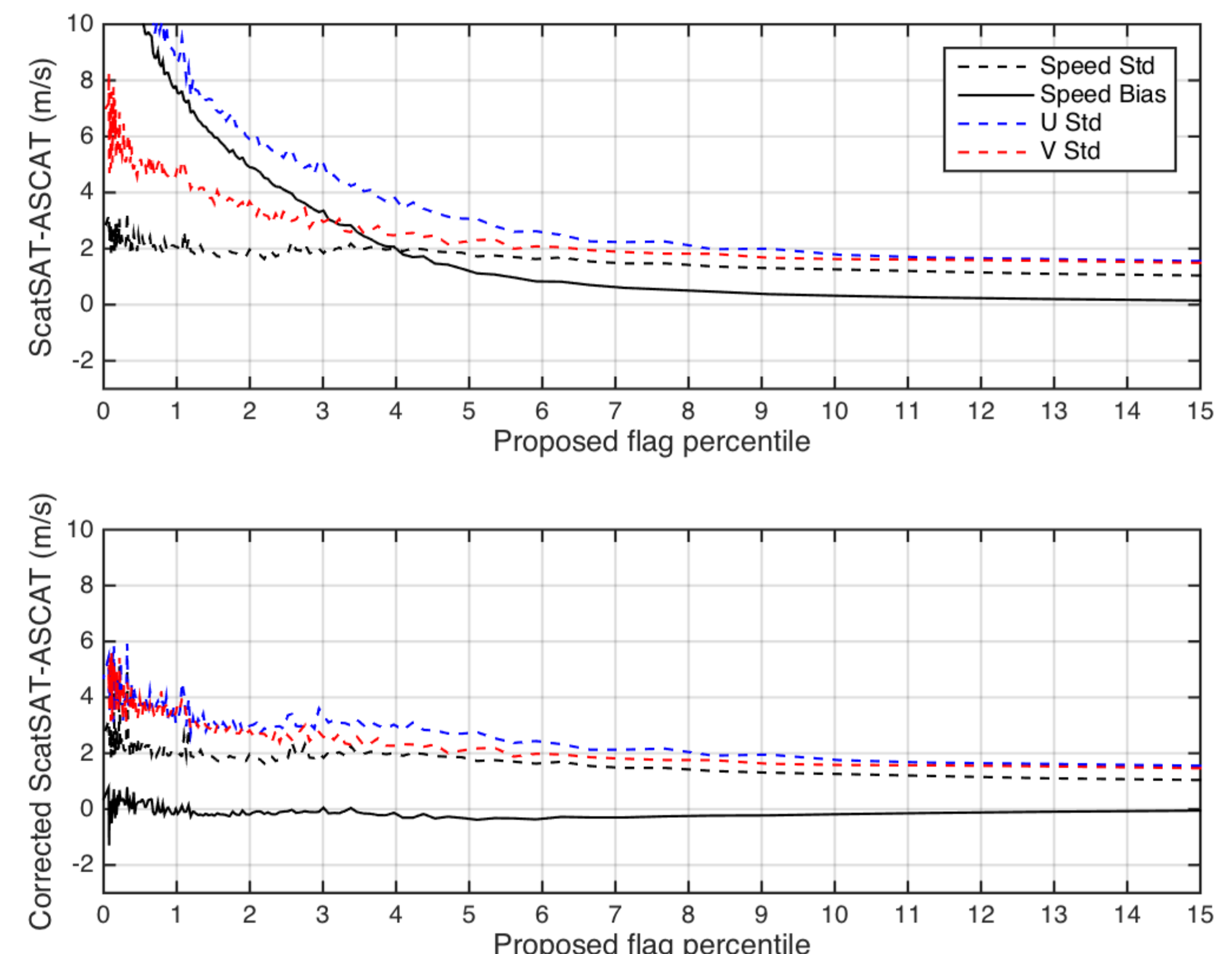


**Figure 4.** Proposed rain flagging and correction performance vs. flag percentile. The flag percentile is obtained from the proposed flag quantity, the absolute value of the estimated Ku-band/C-band speed difference. The corrected speed in the bottom panel is produced using the proposed speed correction.

## References:

- Fore, A. G., B. W. Stiles, A. H. Chau, B. A. Williams, R. S. Dunbar and E. Rodríguez, "Point-Wise Wind Retrieval and Ambiguity Removal Improvements for the QuikSCAT Climatological Data Set," in *IEEE Transactions on Geoscience and Remote Sensing*, vol. 52, no. 1, pp. 51-59, Jan. 2014. doi: 10.1109/TGRS.2012.2235843
- Nie, C. and D. G. Long, "A C-Band Wind/Rain Backscatter Model," in *IEEE Transactions on Geoscience and Remote Sensing*, vol. 45, no. 3, pp. 621-631, March 2007. doi: 10.1109/TGRS.2006.888457
- Stiles, B. W. and R. S. Dunbar, "A Neural Network Technique for Improving the Accuracy of Scatterometer Winds in Rainy Conditions," in *IEEE Transactions on Geoscience and Remote Sensing*, vol. 48, no. 8, pp. 3114-3122, Aug. 2010. doi: 10.1109/TGRS.2010.2049362
- Vogelzang, J., Ad Stoffelen, Scatterometer wind vector products for application in meteorology and oceanography, In *Journal of Sea Research*, Volume 74, 2012, Pages 16-25, ISSN 1385-1101, doi: 10.1016/j.seares.2012.05.002.
- Fernandez, D. E., J. R. Carswell, S. Frasier, P. S. Chang, P. G. Black, and F. D. Marks (2006), Dual-polarized C- and Ku-band ocean backscatter response to hurricane-force winds, *J. Geophys. Res.*, 111, C08013, doi:10.1029/2005JC003048.
- Wang, Z. et al., "SST Dependence of Ku- and C-Band Backscatter Measurements," in *IEEE Journal of Selected Topics in Applied Earth Observations and Remote Sensing*, vol. 10, no. 5, pp. 2135-2146, May 2017, doi: 10.1109/JSTARS.2016.2600749